MUTATION OF THE HEXIM1 GENE RESULTS IN DEFECTS DURING HEART AND VASCULAR DEVELOPMENT PARTLY THROUGH DOWNREGULATION OF VEGF

Monica M. Montano[1], **Yong Qui Doughman**[2], **Huayun Deng**[1], **Laura Chaplin**[1], **Jianqi Yang**[6], **Nancy Wang**[4], **Qiang Zhou**[3], **Nicole L. Ward**[5], and **Michiko Watanabe**[2]

[1]Departments of Pharmacology, University Hospitals of Cleveland, Cleveland, OH 44106

[2]Division of Pediatric Cardiology, Department of Pediatrics, Rainbow Babies and Children's Hospital, University Hospitals of Cleveland, Cleveland, OH 44106

[3]Department of Molecular and Cell Biology, University of California, Berkeley, CA 94720

[4]Department of Pathology, University Hospitals of Cleveland, Cleveland, OH 44106

[5]Department of Dermatology, University Hospitals of Cleveland, Cleveland, OH 44106

[6]Department of Biochemistry, Case Western Reserve University, University Hospitals of Cleveland, Cleveland, OH 44106

Abstract

Our previous studies and those of others indicated that the transcription factor Hexamethylene-bis-acetamide-inducible protein 1 (HEXIM1) is a tumor suppressor and cyclin-dependent kinase inhibitor, and that these HEXIM1 functions are mainly dependent on its C-terminal region. We provide evidence here that the HEXIM1 C-terminal region is critical for cardiovascular development. HEXIM1 protein was detected in the heart during critical time periods in cardiac growth and chamber maturation. We created mice carrying an insertional mutation in the HEXIM1 gene that disrupted its C-terminal region and found that this resulted in prenatal lethality. Heart defects in HEXIM1$_{1-312}$ mice included abnormal coronary patterning and thin ventricular walls. The thin myocardium can be partly attributed to increased apoptosis. Platelet Endothelial Cell Adhesion Molecular Precursor-1 staining of HEXIM1$_{1-312}$ heart sections revealed decreased vascularization of the myocardium despite the presence of coronary vasculature in the epicardium. The expression of Vascular Endothelial Growth Factor (VEGF), known to affect angioblast invasion and myocardial proliferation and survival, was decreased in HEXIM1$_{1-312}$ mice compared to control littermates. We also observed decreased Fibroblast Growth Factor 9 (FGF9) expression, suggesting that effects of HEXIM1 in the myocardium are partly mediated through epicardial FGF9 signaling. Together our results suggest that HEXIM1 plays critical roles in coronary vessel development and myocardial growth. The basis for this role of HEXIM1 is that VEGF is a direct transcriptional target of HEXIM1, and involves attenuation a repressive effects of C/EBPα on VEGF gene transcription.

Address correspondence to: Dr. Monica M. Montano, Case Western Reserve University School of Medicine, Department of Pharmacology, H.G. Wood Bldg. W307, 2109 Adelbert Road, Cleveland, OH 44106 Tel: (216) 368-3378; Fax:(216) 368-3395, mxm126@case.edu.

Keywords

HEXIM1; heart; vascular; development

INTRODUCTION

The transcription factor Hexamethylene-bis-acetamide-inducible protein 1 (HEXIM1) was named for its ability to be upregulated in vascular smooth muscle cells by the differentiating agent Hexamethylene-bis-acetamide (HMBA) [1]. We independently identified HEXIM1 as a novel inhibitor of breast cell growth, Estrogen Down-regulated Gene 1 (EDG1) [2]. Estrogens down-regulate HEXIM1 protein levels, and HEXIM1 inhibits ERα transcriptional activity [2,3]. The mouse homolog of HEXIM1 was cloned as Cardiac Lineage Protein-1 (CLP-1) [4]

Studies using cultured cell lines indicate that HEXIM1 functions as a transcriptional repressor by inhibiting positive transcription elongation factor b (P-TEFb) through its interaction with the cyclin T1 subunit [5,6]. HEXIM1 interacts with 7SK snRNA and forms an inactive P-TEFb complex by binding to and inhibiting the kinase activity of the CDK9 subunit of P-TEFb [5,6]. HEXIM1 interaction with cyclin T1 of P-TEFb is dependent upon the C-terminus of HEXIM1 [5]. Additionally, the region of cyclin T1 where HEXIM1 interacts is within the same region of cyclin T1 where the transcription factors ERα, NF-κB, and c-myc interact, while RNA polymerase II (RNAP II) binds to a different region of cyclin T1 [5-9].

Elevated P-TEFb activity, through overexpression of cyclin T1, was observed in cardiac hypertrophy *in vitro* and *in vivo* [10,11]. Knockout of the HEXIM1 gene resulted in embryo hearts with reduced left ventricular chambers and thickened myocardial walls [12]. Although these results suggested an involvement of P-TEFb and HEXIM1 in cardiac hypertrophy, the relative functional relevance of the interaction of HEXIM1 with P-TEFb vs. other transcription factors in the overall physiological function of HEXIM1 is not well defined and requires further study. Along this line, a recent report indicates HEXIM1 regulation of the Glucocorticoid Receptor that does not involve an interaction with P-TEFb [13].

We now report on the creation and characterization of mice carrying an insertional mutation in HEXIM1, thereby disrupting its C-terminal region. The HEXIM1 mutant protein expressed in our mice was capable of interacting with P-TEFb, similar to what has been shown for a $HEXIM1_{1-314}$ mutant in HeLa cells [14]. Moreover, the $HEXIM1_{1-314}$ mutant was able to inhibit P-TEFb activity. Heart defects was observed in the $HEXIM11_{-312}$ mice, which included abnormal coronary patterning, hypoplasia of myocardial layers of the ventricles, increased chamber size, defects in myocardial vascularization, and increased myocardial apoptosis. We also observed that Vascular Endothelial Growth Factor (VEGF) expression was decreased in $HEXIM1_{1-312}$ hearts compared to control littermates. These indicate that HEXIM1 deficiency affected the VEGF pathway, contributing to dysregulation of coronary vessel development, and influencing myocardial growth.

MATERIALS AND METHODS

Generation of HEXIM1 mutant mice

All animal work reported herein has been approved by the CWRU Institutional Animal Care and Use Committee. A mouse embryonic stem cell line XB322 containing an insertional mutation in HEXIM1 was identified by 5' RACE PCR and inverse PCR in a gene-trapping

screen (Baygenomics, San Francisco, CA ref.[15]). The gene-trapping vector, pGT0pfs, was designed to interrupt genes and to create an in-frame fusion with the β-geo reporter gene. The gene trap vector insertion site was identified using inverse PCR (described in Data Supplement). The XB322 cell line was injected into C57BL/6 blastocysts, and the resulting two chimeric male mice were bred to C57BL/6 females to obtain germline transmission of the mutant allele.

Genotype analyses

Wild type (WT) and mutant alleles were assessed by Southern blot hybridization and/or PCR from DNA isolated from mice tails as described in the Data Supplement.

Histology and Immunohistochemistry

Immunohistochemistry using sections from embryos are described in the Data Supplement. Whole mount PECAM-1 staining is described at http://cbi.swmed.edu/ryburn/sato/htmprotocols/immunowholemount.htm. β-galactosidase staining of whole mounted embryos and embryo sections are described in: http://baygenomics.ucsf.edu/protocols/index.html.

Apoptosis staining

Apoptosis was monitored by terminal deoxynucleotidyltransferase-mediated UTP end labeling (TUNEL) staining using the ApopTag® Peroxidase In Situ Apoptosis Detection Kit (S7100, Chemicon, Temecula, CA).

Cell Culture and Transfections

H9C2 cells were maintained as recommended by ATCC. For northern blot analyses, H9C2 cells were plated onto 100-mm dishes and transfected as previously described [16] using 2 ug expression vector for WT or mutant HEXIM1. Construction of expression vectors for WT and mutant C/EBPα, WT and mutant HEXIM1, and VEGF gene promoter reporter plasmids are described in the Data Supplement. Control and C/EBPα siRNAs (Santa Cruz Biotechnology) were introduced into H9C2 cells using siPORT Amine (Ambion).

Northern Blot Analyses

Total RNA was isolated using Trizol (Invitrogen, Carlsbad, CA) and analyzed using Northern blotting as previously described [16].

Western blot analyses

Western blot experiments were performed as described previously [2]. Membranes were blotted with anti-HEXIM1 antibody or antibody that detects both HEXIM1 and HEXIM2 (Q. Zhou, UC Berkeley) and horseradish peroxidase-conjugated anti-rabbit IgG secondary antibody (GE Healthcare).

In vitro Translation and Protein-protein interaction assays

In vitro transcription and translation of cyclin T1 and WT and mutant C/EBPα were performed using the Promega TNT kit (Promega, Madison, WI). GST-pull down assays were previously described [17]. Construction of vectors encoding full-length and mutant HEXIM1 in frame with glutathione-S-transferase (GST) were previously described [3].

Immunoprecipitation and Chromatin Immunoprecipitation (ChIP) assays

H9C2 cells were transiently transfected with either pCMV-TAG2B-HEXIM1 or pCMV-TAG2B-HEXIM1$_{1-312}$. Immunoprecipitation assays were described previously [3]. ChIP

assays were performed using a modified protocol from Upstate Biotech (Lake Placid, NY) [3] and described in more detail in the Data Supplement. Sequences of primers used in ChIP assays are shown in the Data Supplement.

RESULTS

Generation of HEXIM1 mutant mice

To determine normal physiological function of HEXIM1, we generated HEXIM1 mutant mice using an embryonic stem cell line containing an insertional mutation in the HEXIM1 gene. The mutation resulted in the production of a fusion transcript containing the HEXIM1 sequence encoding the first 312 amino acids of HEXIM1 gene spliced to the β-geo sequence (encoding a fusion β-galactosidase and neomycin phosphotransferase) of the pGTOpfs gene trap vector. Wild type (WT) and mutant alleles were assessed by Southern blot hybridization (Figure 1A) and/or PCR of DNA isolated from mice tails (Figure 1B).

HEXIM1 expression in mice embryos

The fusion of β-geo to the first 312 amino acids of HEXIM1 allowed the expression of β-galactosidase to be controlled by the endogenous HEXIM1 promoter. Thus we used β-galactosidase expression in HEXIM1 heterozygous and homozygous mice to document the pattern of HEXIM1 expression in the embryo heart. β-galactosidase staining of E11.5 embryos indicated nuclear HEXIM1 expression in the myocardium and endothelial lining of the endocardial cushions of the outflow tract, but not in the endothelial lining of the endocardial cushions of the atrioventricular junction (Figure 2A). E17.5 embryos exhibited HEXIM1 expression in the aorta, pulmonary arteries, epicardium, myocardium, inner trabeculae, and endothelium of the endocardial lining (Figure 2B).

The pattern of β-galactosidase expression in the heart of HEXIM1$_{1-312}$ mice correlated with pattern of expression observed with the HEXIM1 antibody in the hearts of WT mice (Figure 2C, see Figure IA in Data Supplement for corresponding western blot). Both staining methods indicated nuclear HEXIM1 expression in the myocardium, with stronger staining evident in the epicardium and in the trabecular myocardium when compared to compact myocardium. Staining using HEXIM1 antibody to the N-terminus of HEXIM1 showed a similar pattern of staining (Figure 2C). HEXIM1 appears to be expressed in epicardial, myocardial, and endocardial cells because β-galactosidase staining was colocalized with cytokeratin 18, sarcomeric actin, and PECAM-1 staining respectively (Data Supplement, Figure IB). Thus, HEXIM1 was expressed in cardiac tissues prior to critical periods in myocardial vascularization and compaction (E13-14).

Mutation of HEXIM1 results in prenatal lethality

To characterize the effect of HEXIM1 mutation on embryo development, timed matings between mice heterozygous for the HEXIM1$_{1-312}$ mutant allele (HEXIM1 het) were performed. At E16.5 and earlier gestational periods, HEXIM1 WT, HEXIM1 het, and HEXIM1$_{1-312}$ mice were viable and recovered at a Mendelian ratio of 1:2:1 (Table 1). However fewer HEXIM1$_{1-312}$ mice than expected were recovered after E16.5.

Abnormal heart development in HEXIM1 mutant mice

Hematoxylin and Eosin (H&E) stained sections of E17.5 mouse embryos indicated that the HEXIM1 mutation resulted in a phenotype with features of dilated cardiomyopathy, an increase in size of the ventricular chambers (relative to heart size), and thin ventricular walls (Figure 3A). The myocardial compact layer was dramatically reduced in the thickness, or regionally lost (sponge like) in HEXIM1$_{1-312}$ hearts (Figure 3B).

Increased apoptosis in the ventricular myocardium of HEXIM1 mutant mice

To determine whether the thinner myocardium was the result of myocyte hypotrophy, hypoplasia, and/or increased apoptosis we examined proliferation and apoptosis in E15.5 embryo hearts. Increased apoptosis, as detected using the Terminal Deoxynucleotidyltransferase-mediated UTP End Labeling (TUNEL) assay, was evident in $HEXIM1_{1-312}$ heart when compared to WT hearts (Figure 3C). TUNEL positive cells costained with the cardiomyocyte marker, sarcomeric actin (Data Supplement, Figure IIA). No difference in proliferation, as detected by Bromodeoxyuridine (BrdU) incorporation, was evident in the left and right ventricle of HEXIM1 mutant mice and WT littermates (Data Supplement, Figure IIB). An increase in proliferation was observed in the intraventricular septum of $HEXIM1_{1-312}$ mice at E15.5, but not at E13.5, when compared to WT littermates.

Abnormal vascular development

Because of the strong expression of HEXIM1 in the epicardium and reports that compaction of subepicardial trabeculations coincides with the invasion of the developing coronary vasculature from the epicardium [18], we examined the effect of HEXIM1 mutation on coronary vessels. WT E15.5 embryos stained for a vascular endothelial cell marker, platelet endothelial cell adhesion molecule precursor (PECAM-1) showed coronary arteries originating from base of the ascending aorta with a regular branching pattern (Figure 4A). In contrast, whole mount PECAM-1 staining of HEXIM1 mutant hearts indicated coronary arteries with a disorganized pattern of branching (Figure 4A). While coronary vasculature was observed in the epicardium, PECAM-1 stained sections revealed that the HEXIM1 mutant heart had markedly decreased vascularization of the myocardium, even with an abundance of coronary vessels in the epicardium (Figure 4A). Together these results suggest that HEXIM1 has an important role in the development of normal coronary vasculature.

Expression of regulators of vascular development

We examined the expression of VEGF, a factor that is known to play an important role in the development of coronary vessels, myocardial vascularization, and myocyte proliferation and survival [19]. In heart sections from E15.5 and E17.5 WT and HEXIM1 mutant embryos, we observed significant decreases in VEGF expression in the ventricular myocardium of HEXIM1 mutant mice (Figure 4B). Western blot analyses also indicated decreased VEGF expression in HEXIM1 mutant hearts (Figure 4D).

In addition to the VEGF family, angiopoietins and Transforming growth factor beta (TGFβ) play major roles in angiogenesis and myocardial vascularization [19]. However, we did not observe differences in the levels of Angiopoietin 1, 2, and 3 and TGFβ in the hearts of WT and HEXIM1 mutant mice (data not shown).

Epicardial and myocardial signaling

HEXIM1 was expressed at the epicardium, endocardium, and myocardium, but more dramatic morphological changes were observed in the compact zone of the myocardium in $HEXIM1_{1-312}$ mice. Considerable evidence support the role of the epicardium and endocardium in the proliferation and vascularization of the myocardium. Thus it is possible that the myocardial defects can be partly attributed to alterations in paracrine signaling to the myocardium in HEXIM1 mutant mice. We were particularly interested in FGFs because of their role not only as a myocyte mitogen but also in promoting coronary vasculogenesis *in vivo* and *in vitro* [20-22]. We observed decreased FGF9 protein expression (Figures 4C and 4D), but no obvious change in FGF2 expression (see Figure III in Data Supplement), in HEXIM1 mutant embryo hearts when compared to WT littermates.

Phenotypic effects of HEXIM1 mutation are not dependent on the ability of HEXIM1 to inhibit RNA polymerase II phosphorylation but involve C/EBPα

We verified cell-autonomous regulation of VEGF expression by HEXIM1 using rat embryo cardiomyoblast H9C2 cells. H9C2 cells, which have low endogenous levels of HEXIM1, were transfected with HEXIM1 expression vectors and VEGF mRNA levels examined. In the developing heart VEGF is expressed by the cardiomyocytes, which is also the major source of VEGF in the heart [23,24]. We observed an increase in VEGF mRNA expression in cells transfected with the WT but not the mutant HEXIM1 expression vector (Figure 5A). Transcriptional regulation of VEGF gene by HEXIM1 is supported by the increase in VEGF promoter reporter activity in H9C2 cells transfected with WT HEXIM1, but not HEXIM1$_{1-312}$, expression vector (Figure 5B). Chromatin Immunoprecipitation (ChIP) experiments indicate that endogenously expressed HEXIM1 is recruited to the -2079/-1252 region of the VEGF promoter region (Figure 6A). We also observed recruitment of HEXIM1$_{1-312}$ to the -2079/-1252 region.

HEXIM1 interacts with 7SK snRNA and form an inactive P-TEFb complex by binding to and inhibiting the kinase activity of the CDK9 subunit of P-TEFb [5,6]. This results in the inhibition of RNAP II phosphorylation. Our *in vitro* GST pull down assays indicated that mutant HEXIM1$_{1-312}$ interacted with cyclin T1 as well as WT HEXIM1 (Data Supplement, Figure IVA). The levels of serine 2 phosphorylated RNAP II were slightly decreased (32%) in HEXIM1$_{1-312}$ mice at E13.5, however this can be attributed to a comparable decrease in total RNAP II levels (Data Supplement, Figure IVB). We did not see a compensatory increase in HEXIM2 expression at E15.5 (Data Supplement, Figure IVC) in response to mutation of HEXIM1. Consistent with HEXIM1 regulation of VEGF expression through a P-TEFb independent mechanism, we observed similar decreases in recruitment of serine 2 phosphorylated RNAP II to the coding sequence of the VEGF gene in H9C2 cells transfected with expression vector for WT HEXIM1 or HEXIM1$_{1-312}$ (Figure 6A). It would then seem paradoxical that HEXIM1 would activate VEGF transcriptional activity while inhibiting serine phosphorylation of RNAPII. However, lack of Ctk1 kinase, the yeast homolog of Cdk9/P-TEFb, leads to loss of CTD Serine 2 phosphorylation but does not obviously affect elongation [25,26], while a Bur1 mutant has defective elongation but apparently normal CTD phosphorylation [27]. CTD Serine 2 phosphorylation is not required for association of elongation factors and studies suggests that other protein-protein interactions are also important [28-30]. It is also likely that some serine 2 phosphorylation occurs through compensatory mechanisms, as detected by immunohistochemistry and western blot analyses (Data Supplement, Figure IVB), but outside the limits of detection of our ChIP assays.

Sequence analyses of the -2079/-1252 region indicated two putative bindings sites for C/EBPα (Data Supplement, Figure VA). We observed binding of C/EBPα to the VEGF gene in cells transfected with expression vector for HEXIM1$_{1-312}$ but not WT HEXMI1 (Figure 6C). Recruitment to the same region of the VEGF promoter may be attributed to an interaction between HEXIM1 and C/EBPα, although we observed weaker interaction of HEXIM1$_{1-312}$ with C/EBPα (Figure 6B). The implication from the results of these studies is that WT HEXIM1 is able to displace C/EBPα from the VEGF promoter, and thus mediate release from C/EBPα repressive action. Due to the weaker interaction of HEXIM1$_{1-312}$ with C/EBPα, HEXIM1$_{1-312}$ is not able to attenuate the inhibitory action of C/EBPα on VEGF gene transcription. Opposing actions of C/EBPα and HEXIM1 is supported by our observation that increased expression of C/EBPα resulted in inhibition of the ability of HEXIM1 to upregulate VEGF promoter reporter activity (Figure 6C). The interaction of HEXIM1 with the C/EBPα is also disrupted by deletion of HEXIM1 N-terminus (Figure 6C). C-terminus of C/EBPα mediates the interaction with HEXIM1 (Data Supplement, Figure VB). No change in SP1 recruitment was observed in cells transfected with expression

vector for WT or mutant HEXIM1 (Figure 6C). HEXIM1 regulation of VEGF gene transcription may also be independent of HIF-1α because HEXIM1 did not activate a luciferase reporter containing the HIF-1α response element within the -944/633 region of the VEGF gene (Figure 5B). HEXIM1 was not recruited to the -944/-633 region (Figure 6A).

Our ChIP data implicate C/EBPα as a negative regulator of VEGF expression. This is further supported by the increase in VEGF mRNA levels as a result of downregulation of C/EBPα levels using C/EBPα siRNA (Figure 6C). More importantly, hearts collected from C/EBPα knockout mice (described in ref. [31] and Data Supplement) had increased VEGF expression when compared to WT hearts (Figure 6D). Together our data support P-TEFb independent regulation of VEGF by HEXIM1 that involves HEXIM1-mediated attenuation of an inhibitory effect of C/EBPα on VEGF expression.

DISCUSSION

To further characterize the physiological functions of HEXIM1, we created mice carrying an insertional mutation in HEXIM1, thereby disrupting its functionally important C-terminal region. Histology and immunohistochemistry revealed heart defects in HEXIM1$_{1-312}$ mice that included hypoplasia of myocardial layers, abnormal coronary patterning, increased chamber size and decreased heart rate. Angioblast invasion from the epicardium is mediated by FGFs and VEGF [32]. Our results showed that both FGF9 and VEGF expression was decreased in HEXIM1$_{1-312}$ hearts compared to control littermates. However the decrease in VEGF expression occur prior to formation of the epicardium and changes in FGF9 expression. Moreover, our studies indicated that VEGF is a direct transcriptional target of HEXIM1, contributing to regulation of coronary vessel development and influencing myocardial growth. Thus HEXIM1 regulation of myocardial signaling may play the primary role, relative to HEXIM1 regulation of epicardial signaling, in cardiovascular development. HEXIM1 regulation of VEGF involves the transcription factor C/EBPα, and to our knowledge this is the first report of negative regulation of VEGF by C/EBPα in the heart.

We saw a decrease in FGF9 in the myocardium, an important factor in epicardial-myocardial signaling [20]. Epicardial and endocardial FGF9 signaling are essential for myocardial proliferation and differentiation *in vivo* [20]. FGF9 signaling to the cardiomyoblast is also essential for coronary development. Thus FGF9 can also indirectly regulate myocardial proliferation through VEGF [33]. Redundancy in regulation of VEGF is not surprising giving the importance of maintaining VEGF at certain levels during heart development.

Signaling between the epicardium and myocardium, as well as endocardium and myocardium, are bidirectional (reviewed in ref. [23]). The extent of vascularization corresponds to the rate of myocardial growth and the ratio of compact-to-spongious myocardium. As the myocardial wall matures and myocytes orient along particular axes, capillaries also align along the same axes as do myocytes (reviewed in ref. [34]). Thus, it is also likely that HEXIM1-mediated signaling from the myocardium influences coronary vessel development. It is possible that the abnormal branching observed in coronary vessel in the epicardium can be attributed to defective signaling from the myocardium and/or misalignment of myocytes in HEXIM1 mutant mice. Along this line, restoration of Friend of GATA 2 (FOG-2) expression in cardiac myocytes by cardiac specific alpha myosin heavy chain promoter in the FOG-2 null mice led to the development of normal coronary vasculature [35]. The selective restoration or knockout of HEXIM1 in the epicardium or the myocardium is important in defining in which tissues HEXIM1-mediated signaling is required for normal cardiac development.

The development of a mature coronary circulation and the establishment of a myocardial capillary vascular plexus are relatively late prenatal events (E13-E14 in mice) and defects in these processes are consistent with lethality at later gestational periods of the HEXIM1 mutant mice. Angioblasts for the coronary vasculature arise partly by induction of epithelial to mesenchymal transformation of cells originating from the splanchnic mesoderm (reviewed in ref. [32]). VEGF does not appear to be involved in angioblast induction, but is believed to be an important mediator of angioblast invasion. VEGF expression is driven by hypoxia in many cell types and tissues studied so far (reviewed in ref. [36]). Our results are consistent with HEXIM1 as another regulator of VEGF induction of myocardial vascularization. Furthermore HEXIM1 regulation HEXIM1 involves attenuation of an inhibitory effect of C/EBPα on VEGF expression. There are no reports to support that HEXIM1 binds directly to DNA thus it is unlikely that C/EBPα and HEXIM1 compete for DNA binding. Our findings suggest that HEXIM1 interaction with C/EBPα results in the removal of C/EBPα from the VEGF promoter (see Figure VI in Data Supplement for our working model).

Similar to our findings, mice harboring null alleles of the HEXIM1 were not represented in the normal Mendelian ratio past E16.5 [12]. However in contrast to our results, HEXIM1-/- fetal hearts exhibited reduced left ventricular chamber with thickened myocardial walls, features suggestive of cardiac hypertrophy. Contractile and non-contractile protein genes known to be re-expressed during cardiac hypertrophy had higher expression levels in HEXIM1-/- hearts thereby confirming the hypertrophic phenotype at the molecular level. The hypertrophic phenotype of the HEXIM1-/- mice is consistent with the findings that overexpression of the cyclin T1 subunit resulted in a hypertrophic phenotype *in vitro* and *in vivo* [10,11].

Our results however indicated that HEXIM1 has important physiological functions that were not dependent on its ability to interact with and inhibit P-TEFb, and may explain the differences in phenotypic effects of HEXIM1 null mutation and mutation of HEXIM1 in our mouse model. However pathological hypertrophy eventually degenerates to dilated cardiomyopathy and the process may merely be accelerated in our HEXIM1 mutant mice. In the HEXIM1 null mice, any effects on myocardial vascularization/growth are perhaps initially counterbalanced by induction of hypertrophy resulting from activation of CDK9. An alternative model is that WT and mutant HEXIM1 differentially regulates HEXIM1 target genes by differentially regulating transcription factors such as C/EBPα.

The effects of mutating HEXIM1 were specific as shown by our results. We also did not see effects on the level of expression of other transcription factors such as Nkx2.5, GATA4, MEF2A, and SRF1 (data not shown), which are well known to play important roles in heart development. It is unlikely that our findings can be attributed to compensatory upregulation of the recently discovered isoform of HEXIM1, HEXIM2 [37,38], because we did not see a change in HEXIM2 expression in HEXIM1 mutant mice. However we cannot rule out other compensatory mechanisms.

Supplementary Material

Refer to Web version on PubMed Central for supplementary material.

Acknowledgments

REFERENCES

1. Kusuhara M, Nagasaki K, Kimura K, Maass N, Manabe T, Ishikawa S, Aikawa M, Miyazaki K, Yamaguchi K. Cloning of Hexamethylene-bis-acetamide-inducible transcript, HEXIM1, in human vascular smooth muscle cells. Biomedical Res 1999;20:273–279.

2. Wittmann BM, Wang N, Montano MM. Identification of a novel inhibitor of cell growth that is down-regulated by estrogens and decreased in breast tumors. Cancer Res 2003;63:5151–5158. [PubMed: 12941847]

3. Wittmann BM, Fujinaga K, Deng H, Ogba N, Montano MM. The breast cell growth inhibitor, estrogen down regulated gene 1, modulates a novel functional interaction between estrogen receptor alpha and transcriptional elongation factor cyclin T1. Oncogene 2005;24:5576–5588. [PubMed: 15940264]

4. Huang F, Wagner M, Siddiqui MA. Structure, expression, and functional characterization of the mouse CLP-1 gene. Gene 2002;292:245–259. [PubMed: 12119119]

5. Michels AA, Nguyen VT, Fraldi A, Labas V, Edwards M, Bonnet F, Lania L, Bensaude O. MAQ1 and 7SK RNA interact with CDK9/CyclinT complexes in a transcription – dependent manner. Mol Cell Biol 2003;23:4859–4869. [PubMed: 12832472]

6. Yik JH, Chen R, Nishimura R, Jennings JL, Link AJ, Zhou Q. Inhibition of P-TEFb (CDK9/Cyclin T) kinase and RNA polymerase II transcription by the coordinated actions of HEXIM1 and 7SK snRNA. MolCell 2003;12:971–982.

7. Fong YW, Zhou Q. Relief of two built-In autoinhibitory mechanisms in P-TEFb is required for assembly of a multicomponent transcription elongation complex at the human immunodeficiency virus type 1 promoter. Mol Cell Biol 2000;20:5897–5907. [PubMed: 10913173]

8. Kanazawa S, Soucek L, Evan G, Okamoto T, Peterlin BM. c-Myc recruits P-TEFb for transcription, cellular proliferation and apoptosis. Oncogene 2003;22:5707–5711. [PubMed: 12944920]

9. Barboric M, Nissen RM, Kanazawa S, Jabrane-Ferrat N, Peterlin BM. NF-kB binds P-TEFb to stimulate transcriptional elongation by RNA polymerase II. Mol Cell 2001;8:327–337. [PubMed: 11545735]

10. Sano M, Abdellatif M, Oh H, Xie M, Bagella L, Giordano A, Michael LH, DeMayo FJ, Schneider MD. Activation and function of cyclin T-Cdk9 (positive transcription elongation factor-b) in cardiac muscle-cell hypertrophy. Nat Med 2002;8:1310–1317. [PubMed: 12368904]

11. Sano M, Wang SC, Shirai M, Scaglia F, Xie M, Sakai S, Tanaka T, Kulkarni PA, Barger PM, Youker KA, Taffet GE, Hamamori Y, Michael LH, Craigen WJ, Schneider MD. Activation of cardiac Cdk9 represses PGC-1 and confers a predisposition to heart failure. EMBO J 2004;23:3559–3569. [PubMed: 15297879]

12. Huang F, Wagner M, Siddiqui MA. Ablation of the CLP-1 gene leads to down-regulation of the HAND1 gene and abnormality of the left ventricle of the heart and fetal death. Mech Dev 2004;121:559–572. [PubMed: 15172687]

13. Shimizu N, Ouchida R, Yoshikawa N, Hisada T, Watanabe H, Okamoto K, Kusuhara M, Handa H, Morimoto C, Tanaka H. HEXIM1 forms a transcriptionally abortive complex with glucocorticoid receptor without involving 7SK RNA and positive transcription elongation factor b. Proc Natl Acad Sci 2005;102:8555–8560. [PubMed: 15941832]

14. Blazek D, Barboric M, Kohoutek J, Oven I, Peterlin BM. Oligomerization of HEXIM1 via 7SK snRNA and coiled-coil region directs the inhibition of P-TEFb. Nucleic Acids Res 2005;33:7000–7010. [PubMed: 16377779]

15. Stryke D, Kawamoto M, Huang CC, Johns SJ, King LA, Harper CA, Meng EC, Lee RE, Yee A, L'Italien L, Chuang PT, Young SG, Skarnes WC, Babbitt PC, Ferrin TE. BayGenomics: a resource of insertional mutations in mouse embryonic stem cells. Nucleic Acids Res 2003;31:278–281. [PubMed: 12520002]

16. Montano MM, Katzenellenbogen BS. The quinone reductase gene: a unique estrogen receptor-regulated gene that is activated by antiestrogens. Proc Natl Acad Sci 1997;94:2581–2586. [PubMed: 9122238]

17. Montano MM, Ekena K, Delage-Mourroux R, Chang W, Martini P, Katzenellenbogen BS. An estrogen receptor-selective coregulator that potentiates the effectiveness of antiestrogens and represses the activity of estrogens. Proc Natl Acad Sci 1999;96:6947–6952. [PubMed: 10359819]

18. Weiford BC, Subbarao VD, Mulhern KM. Noncompaction of the ventricular myocardium. Circulation 2004;109:2965–2971. [PubMed: 15210614]

19. Majesky MW. Development of coronary vessels. Curr Top Dev Biol 2004;62:225–259. [PubMed: 15522744]

20. Lavine KJ, Yu K, White AC, Zhang X, Smith C, Partanen J, Ornitz DM. Endocardial and epicardial derived FGF signals regulate myocardial proliferation and differentiation in vivo. DevCell 2005;8:85–95.

21. Mikawa T. Retroviral targeting of FGF and FGFR in cardiomyocytes and coronary vascular cells during heart development. Ann N Y Acad Sci 1995;752:506–516. [PubMed: 7755295]

22. Mima T, Ueno H, Fischman DA, Williams LT, Mikawa T. Fibroblast growth factor receptor is required for in vivo cardiac myocyte proliferation at early embryonic stages of heart development. Proc Natl Acad Sci 1995;92:467–471. [PubMed: 7831312]

23. Brutsaert DL. Cardiac endothelial-myocardial signaling: its role in cardiac growth, contractile performance, and rhythmicity. Physiol Rev 2003;83:59–115. [PubMed: 12506127]

24. Giordano FJ, Gerber HP, Williams SP, VanBruggen N, Bunting S, Ruiz-Lozano P, Gu Y, Nath AK, Huang Y, Hickey R, Dalton N, Peterson KL, Ross J Jr, Chien KR, Ferrara N. A cardiac myocyte vascular endothelial growth factor paracrine pathway is required to maintain cardiac function. Proc Natl Acad Sci 2001;98:5780–5785. [PubMed: 11331753]

25. Ahn SH, Kim M, Buratowski S. Phosphorylation of serine 2 within the RNA polymerase II C-terminal domain couples transcription and 3' end processing. Mol Cell 2004;13:67–76. [PubMed: 14731395]

26. Cho EJ, Kobor MS, Kim M, Greenblatt J, Buratowski S. Opposing effects of Ctk1 kinase and Fcp1 phosphatase at Ser 2 of the RNA polymerase II C-terminal domain. Genes Dev 2001;15:3319–3329. [PubMed: 11751637]

27. Keogh MC, Podolny V, Buratowski S. Bur1 kinase is required for efficient transcription by RNA polymerase II. Mol Cell Biol 2003;23:7005–7018. [PubMed: 12972617]

28. Krogan NJ, Kim M, Ahn SH, Zhong G, Kobor MS, Cagney G, Emili A, Shilatifard A, Buratowski S, Greenblatt JF. RNA polymerase II elongation factors of Saccharomyces cerevisiae: a targeted proteomics approach. Mol Cell Biol 2002;22:6979–6992. [PubMed: 12242279]

29. Lindstrom DL, Squazzo SL, Muster N, Burckin TA, Wachter KC, Emigh CA, McCleery JA, Yates JR 3rd, Hartzog GA. Dual roles for Spt5 in pre-mRNA processing and transcription elongation revealed by identification of Spt5-associated proteins. Mol Cell Bio 23:1368–1378. [PubMed: 12556496]

30. Squazzo SL, Costa PJ, Lindstrom DL, Kumer KE, Simic R, Jennings JL, Link AJ, Arndt KM, Hartzog GA. The Paf1 complex physically and functionally associates with transcription elongation factors in vivo. EMBO J 2002;21:1764–1774. [PubMed: 11927560]

31. Yang J, Croniger CM, Lekstrom-Himes J, Zhang P, Fenyus M, Tenen DG, Darlington GJ, Hanson RW. Metabolic response of mice to a postnatal ablation of CCAAT/enhancer-binding protein alpha. J Biol Chem 2005;280:38689–38699. [PubMed: 16166091]

32. Poole TJ, Finkelstein EB, Cox CM. The role of FGF and VEGF in angioblast induction and migration during vascular development. Dev Dyn 2001;220:1–17. [PubMed: 11146503]

33. Lavine KJ, White AC, Park C, Smith CS, Choi K, Long F, Hui CC, Ornitz DM. Fibroblast growth factor signals regulate a wave of Hedgehog activation that is essential for coronary vascular development. Genes Dev 2006;20:1651–1666. [PubMed: 16778080]

34. Wada AM, Willet SG, Bader D. Coronary vessel development: a unique form of vasculogenesis. Arterioscler Thromb Vasc Biol 2003;23:2138–2145. [PubMed: 14525796]

35. Tevosian SG, Deconinck AE, Tanaka MS, chinke M, Litovsky SH, Izumo S, Fujiwara Y, Orkin SH. FOG-2, a cofactor for GATA transcription factors, is essential for heart morphogenesis and development of coronary vessels from epicardium. Cell 2000;101:729–739. [PubMed: 10892744]

36. Tomanek RJ, Lotun K, Clark EB, Suvarna PR, Hu N. VEGF and bFGF stimulate myocardial vascularization in embryonic chick. Am J Physiol 1998;274:H1620–H1626. [PubMed: 9612372]

37. Yik JH, Chen R, Pezda AC, Zhou Q. Compensatory contributions of HEXIM1 and HEXIM2 in maintaining the balance of active and inactive positive transcription elongation factor b complexes for control of transcription. J Biol Chem 2005;280:16368–16376. [PubMed: 15713661]

38. Byers SA, Price JP, Cooper JJ, Li Q, Price DH. HEXIM2, a HEXIM1-related protein, regulates positive transcription elongation factor b through association with 7SK. J Biol Chem 2005;180:16360–16367. [PubMed: 15713662]
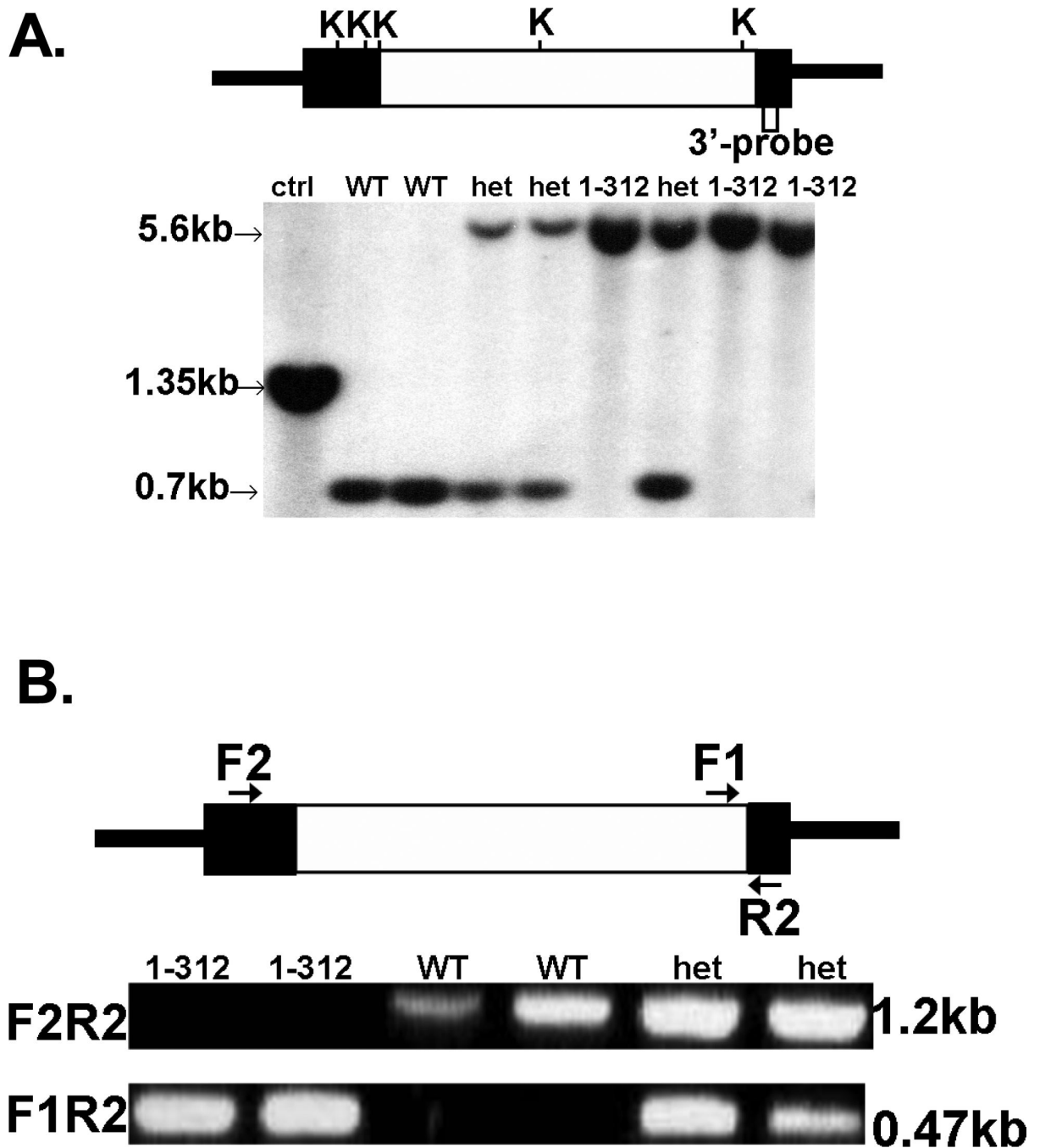
Figure 1. Genotype analyses of HEXIM1 mutant mice
(A) The upper panel shows insertion of the gene trap vector into the mouse HEXIM1 gene, resulting in the mutant HEXIM1 allele. The insertion also resulted in an in-frame fusion with the β-geo (encoding β-galactosidase and neomycin phosphotransferase) reporter gene. The lower panel shows a Southern blot wherein genomic DNA was digested with *Kpn*I (K) restriction enzyme and analyzed by hybridization with a 3' end probe. (B) PCR genotyping of tail DNA from E17.5 embryos. F1, F2, and R2 refer to PCR primers (see Data Supplement for primer sequences).

A. E11.5
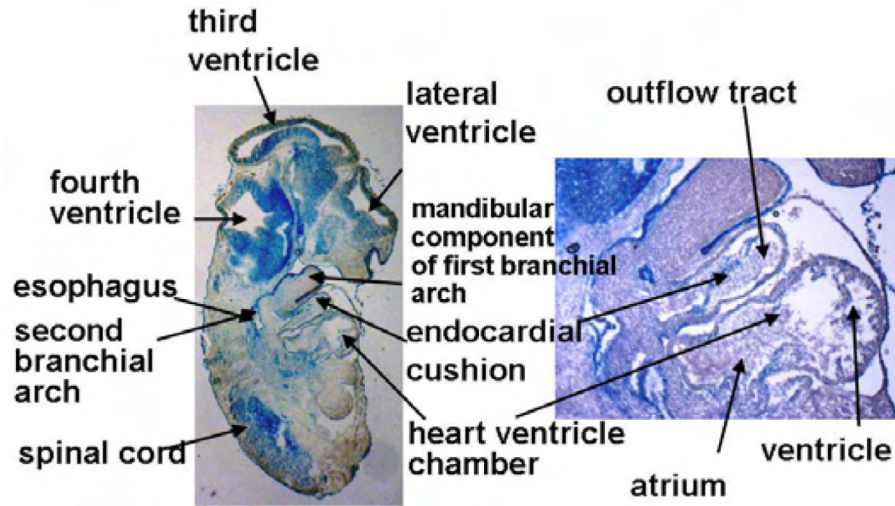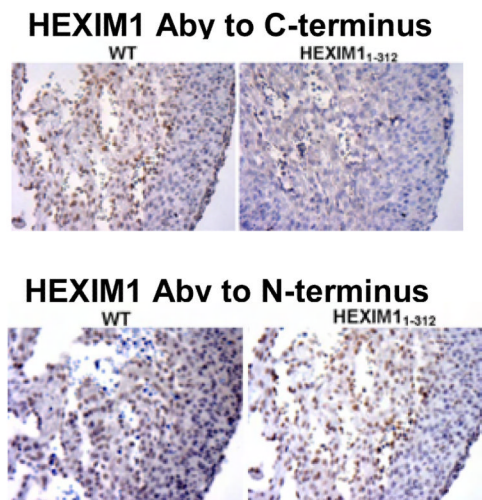

B. E17.5
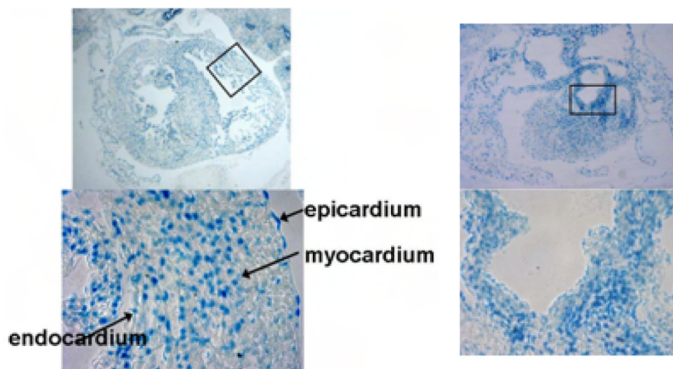
C. E13.5

Figure 2. Expression of HEXIM1 in embryo hearts
(A) β-galactosidase staining of sections from E11.5 embryos (B) Cross sections of E17.5 embryos stained for β-galactosidase. (C) Staining of tissue sections from E13.5 WT and mutant embryos were performed using HEXIM1 antibody to the C-terminal or N-terminal region of HEXIM1.
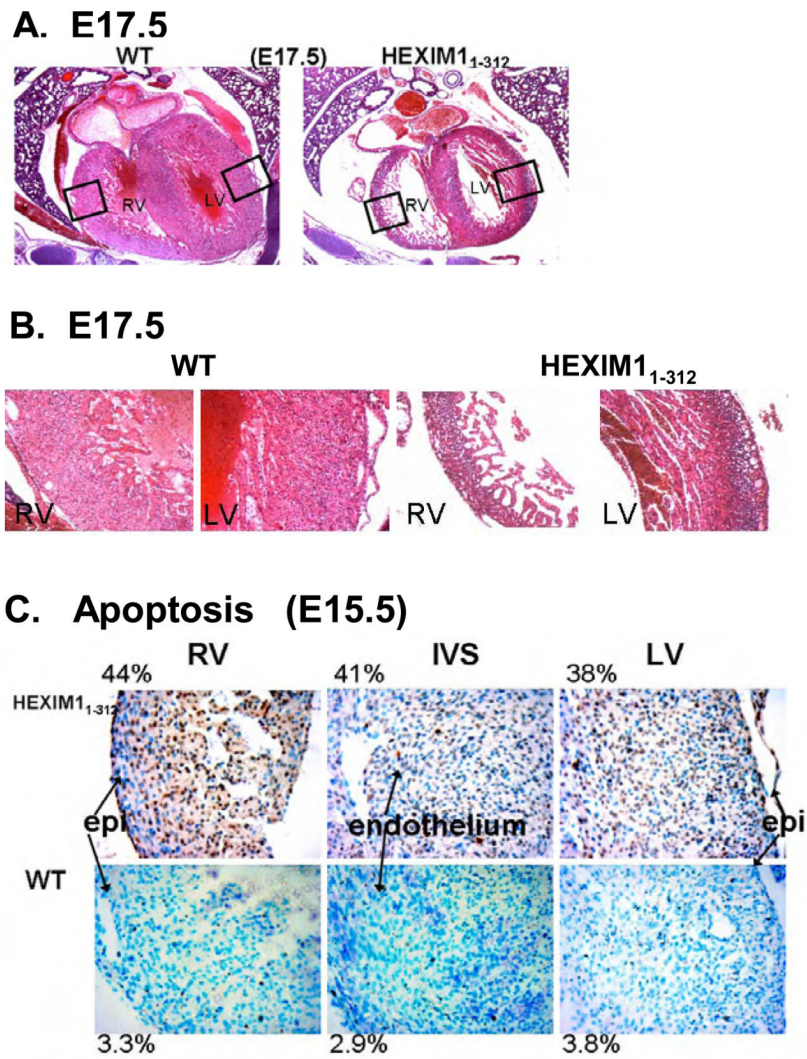
Figure 3. HEXIM1 mutation resulted in features similar to dilated cardiomyopathy and increased apoptosis in the ventricular myocardium
(A) H&E stained sections of E17.5 mutant HEXIM1 embryos. (B) Higher power view (C) Increased apoptosis was evident in the wall of the left and right ventricular myocardium and intraventricular septum of HEXIM1$_{1-312}$ mice at E15.5. LV=left ventricle; RV=right ventricle; IVS=intraventricular septum.

A. PECAM-1 (E15.5)

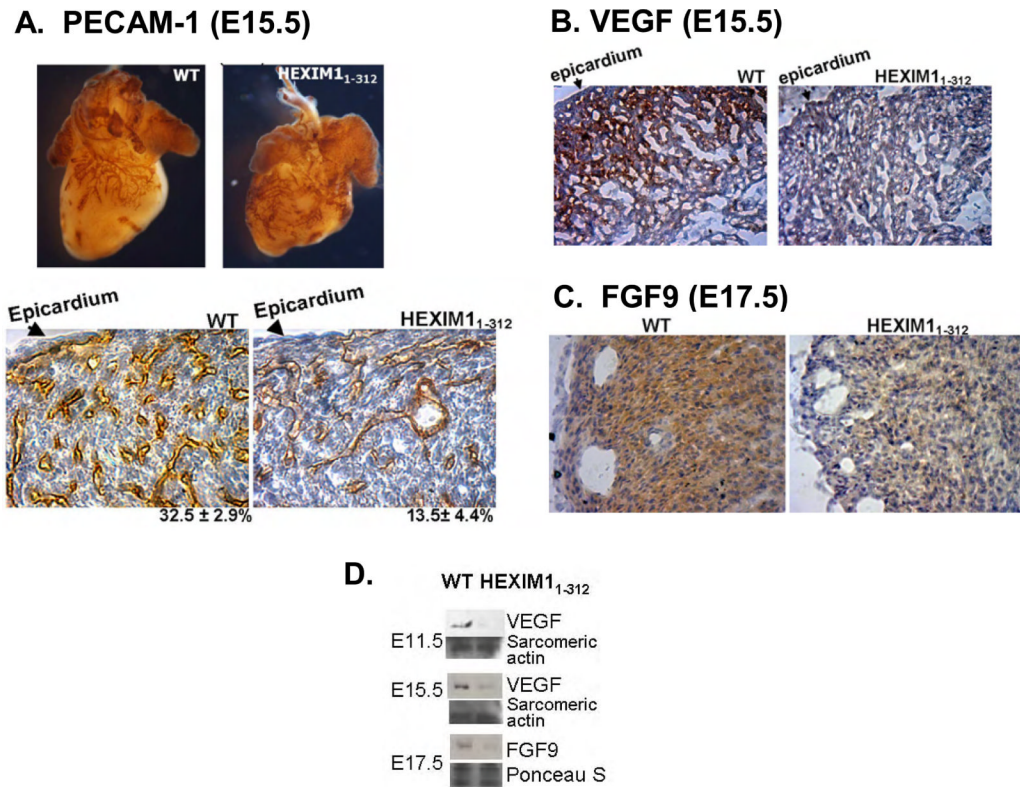## B. VEGF (E15.5)

C. FGF9 (E17.5)

D.

Figure 4. Aberrant coronary vessel formation and differentiation and decreased VEGF and FGF9 expression in HEXIM1 mutant mice
(A) PECAM-1 immunostaining of E15.5 WT and HEXIM1 mutant whole-mounted embryos and heart sections. (B) The hearts of E15.5 WT and HEXIM1 mutant mice were immunostained with VEGF antibody. (C) Immunostaining of the hearts of E17.5 WT and HEXIM1 mutant mice with FGF9 antibody. (D) VEGF and FGF9 expression were also determined using western blot analyses.
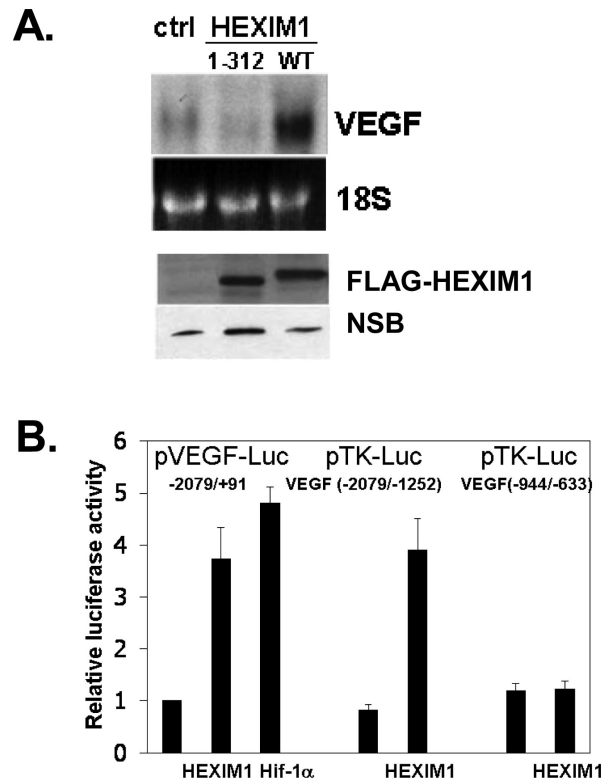
Figure 5. Regulation of VEGF expression by HEXIM1
(A) Northern blot analyses of VEGF expression in H9C2 cells transfected with control vector or expression vectors for WT or mutant HEXM1$_{1-312}$. The 18S ribosomal band was used to normalize for unequal loading. The autoradiograph is representative of 3 experiments. The lower panels show Western blot analyses of WT and mutant HEXIM1 expression using the FLAG antibody. NSB = non-specific band. (B) H9C2 cells were transfected with an expression vector for HEXIM1 and luciferase reporter gene containing VEGF gene promoter. The cells were also transfected with a Renilla luciferase internal control plasmid to normalize for transfection efficiency. Fold activation over cells transfected with control expression vector is displayed as an average of three independent experiments.
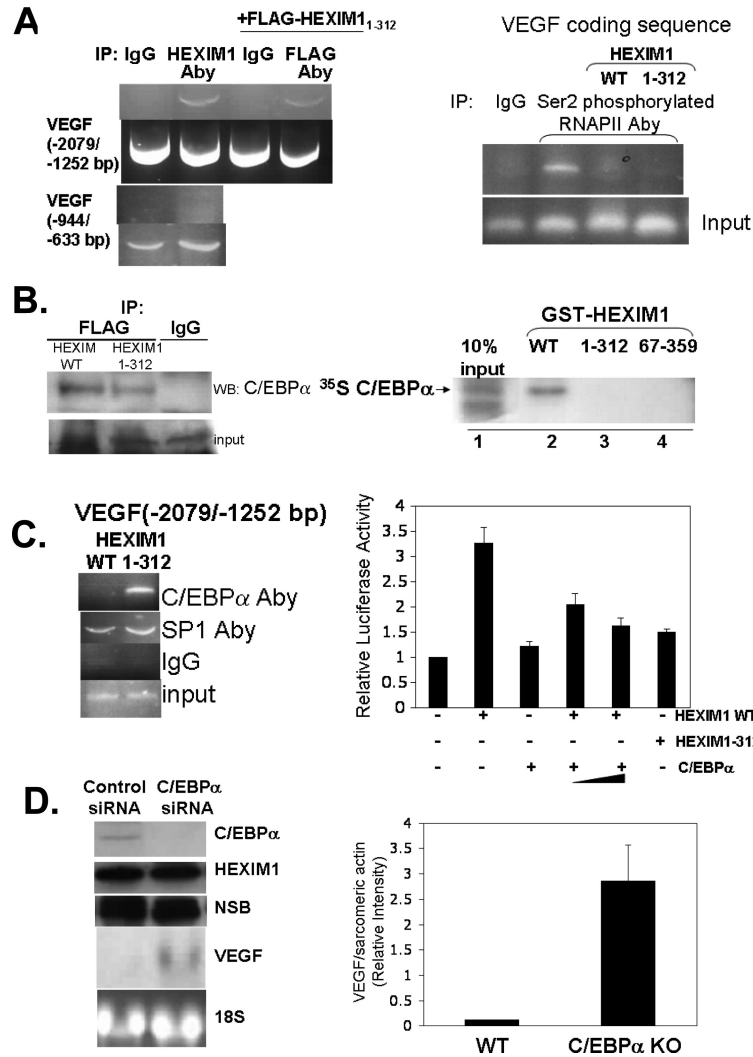
Figure 6. VEGF is a direct transcriptional target of HEXIM1

(A) H9C2 cells were transfected with control or expression vector for HEXIM$_{1-312}$ and subjected to ChIP assays. The -2079/-1252, -944/-633, and coding sequence regions of VEGF gene promoter were immunoprecipitated with HEXIM1 (B) (left) H9C2 cells were transfected with expression vector for WT HEXIM1 or HEXIM$_{1-312}$ and subjected to ChIP assays. The coding sequence region of VEGF gene promoter was immunoprecipitated with serine 2 phosphorylated RNAPII (right). (B) For IP experiments (left), WT and mutant HEXIM1 were immunoprecipitated from equal concentrations of whole cell extracts using FLAG polyclonal antibody followed by Western blotting with anti-C/EBPα. Normal rabbit IgG was used as control. "Input" lane represents 10% of the total volume of lysate used in each reaction. For GST-pull down assays (right) equal amounts each of *in vitro* translated and [^{35}S]methionine-labeled WT C/EBPα were incubated with equal amounts each of either glutathione-S-transferase (GST) control, WT or mutant HEXIM1. "Input" lane represents 10% of the total volume of *in vitro* translated product used in each reaction. (C) (left) The -2079/-1252 region of VEGF gene promoter was immunoprecipitated with C/EBPα or SP1 antibodies. The "input control" represents PCR for 2% of total chromatin used in each reaction. (right) H9C2 cells were transfected with expression vectors for WT HEXIM1, HEXIM1$_{1-312}$, and C/EBPα, and luciferase reporter gene containing the -2079/-1252 region of the VEGF gene promoter. (D) VEGF expression in (left) H9C2 cells transfected with

control and C/EBPα siRNA using Northern blot analyses and in (right) WT (n=7) and C/EBPα (n=7) knockout mice using Western blot analyses. Densitometric quantifications of VEGF protein expression levels were expressed relative to expression levels of sarcomeric actin. NSB = non-specific band.

Table 1

| Stage | Total | Genotype | | Expected vs. Observed Ratios (X^2, p values) |
		+/+	Heterozygotes	HEXIM1$_{1-312}$	
E11.5	95	27 (28%)	46 (48%)	22 (23%)	0.73
E16.5	77	18 (23%)	43 (56%)	16 (21%)	0.56
E17.5	120	39 (33%)	62 (52%)	19 (16%)	0.03
E18.5	56	16 (29%)	34 (61%)	6 (11%)	0.05